

## Point, surface and volumetric heat sources in the thermal modelling of selective laser melting

Yang, Yabin; Ayas, Can

**DOI**

[10.1063/1.5008032](https://doi.org/10.1063/1.5008032)

**Publication date**

2017

**Document Version**

Final published version

**Published in**

Proceedings of the 20th International ESAFORM Conference on Material Forming (ESAFORM 2017)

**Citation (APA)**

Yang, Y., & Ayas, C. (2017). Point, surface and volumetric heat sources in the thermal modelling of selective laser melting. In D. Brabazon, S. Naher, & I. Ul Ahad (Eds.), *Proceedings of the 20th International ESAFORM Conference on Material Forming (ESAFORM 2017)* Article 040006 (AIP Conference Proceedings; Vol. 1896, No. 1). AIP Publishing. <https://doi.org/10.1063/1.5008032>

**Important note**

To cite this publication, please use the final published version (if applicable).  
Please check the document version above.

**Copyright**

Other than for strictly personal use, it is not permitted to download, forward or distribute the text or part of it, without the consent of the author(s) and/or copyright holder(s), unless the work is under an open content license such as Creative Commons.

**Takedown policy**

Please contact us and provide details if you believe this document breaches copyrights.  
We will remove access to the work immediately and investigate your claim.

# Point, surface and volumetric heat sources in the thermal modelling of selective laser melting

Yabin Yang, and Can Ayas

Citation: [AIP Conference Proceedings](#) **1896**, 040006 (2017);

View online: <https://doi.org/10.1063/1.5008032>

View Table of Contents: <http://aip.scitation.org/toc/apc/1896/1>

Published by the [American Institute of Physics](#)

---

## Articles you may be interested in

[Computationally efficient thermal-mechanical modelling of selective laser melting](#)

[AIP Conference Proceedings](#) **1896**, 040005 (2017); 10.1063/1.5008031

[Numerical simulation of complex part manufactured by selective laser melting process](#)

[AIP Conference Proceedings](#) **1896**, 040013 (2017); 10.1063/1.5008039

[Laser powder bed fusion additive manufacturing of metals; physics, computational, and materials challenges](#)

[Applied Physics Reviews](#) **2**, 041304 (2015); 10.1063/1.4937809

[Analysis of laser–melt pool–powder bed interaction during the selective laser melting of a stainless steel](#)

[Journal of Laser Applications](#) **29**, 022303 (2017); 10.2351/1.4983259

---

# Point, Surface and Volumetric Heat Sources in the Thermal Modelling of Selective Laser Melting

Yabin Yang<sup>1,a)</sup> and Can Ayas<sup>1,b)</sup>

<sup>1</sup>*Structural Optimization and Mechanics Group, Department of Precision and Microsystems Engineering, Faculty of Mechanical, Maritime and Material Engineering, Delft University of Technology, Mekelweg 2, 2628 CD, Delft, The Netherlands*

<sup>a)</sup>Corresponding author: Y.Yang-6@tudelft.nl

<sup>b)</sup>C.Ayas@tudelft.nl

**Abstract.** Selective laser melting (SLM) is a powder based additive manufacturing technique suitable for producing high precision metal parts. However, distortions and residual stresses within products arise during SLM because of the high temperature gradients created by the laser heating. Residual stresses limit the load resistance of the product and may even lead to fracture during the built process. It is therefore of paramount importance to predict the level of part distortion and residual stress as a function of SLM process parameters which requires a reliable thermal modelling of the SLM process. Consequently, a key question arises which is how to describe the laser source appropriately. Reasonable simplification of the laser representation is crucial for the computational efficiency of the thermal model of the SLM process. In this paper, first a semi-analytical thermal modelling approach is described. Subsequently, the laser heating is modelled using point, surface and volumetric sources, in order to compare the influence of different laser source geometries on the thermal history prediction of the thermal model. The present work provides guidelines on appropriate representation of the laser source in the thermal modelling of the SLM process.

## INTRODUCTION

Selective laser melting (SLM) is a common additive manufacturing technique for producing metal parts with mechanical properties similar to those made by traditional manufacturing methods. However, SLM allows for higher topological freedom when compared to manufacturing techniques such as casting, milling, drawing and CNC. One of the critical issues associated with SLM is the distortion of the part and generation of residual stresses during the process. Part distortions and residual stresses arise due to the high temperature gradients created by the localised laser heating and subsequent cooling [1, 2]. Therefore, accurate prediction of these field quantities requires a valid prediction of the temperature history. Since laser beam is the source of energy in SLM, a reasonable description of the laser heating is a necessity.

Generally, the laser scanning line can be discretised into finite number of heat sources along the scanning vector. For each heat source, a Gaussian distribution of the laser intensity is usually assumed in the plane of scanning [3, 4]. Moreover, along the out of plane direction, the laser energy also decreases [3] as a result of the powder-bed laser interaction. Therefore, a laser scanning vector employed in SLM is well described with a set of 3-dimensional heat sources located along the scanning vector. However, the dimension of the laser spot is typically tens of micrometers, while the part produced has dimensions on the order of millimetres. This mismatch between the characteristic length scales of the problem requires an extremely fine discretisation of the domain upon solving the heat equation with a standard numerical method such as finite elements (FE).

As a first level of simplification a volumetric source can be treated as a surface source, neglecting the laser penetration depth into the powder-bed [5]. The next level simplification assumes a negligible radius of the laser spot within the scanning plane, and thus a finite number of point heat sources become appropriate to represent a laser scan vector. Although such simplifications will considerably improve the computational efficiency, overall temperature history should be sufficiently insensitive for these simplifications in order not to compromise accuracy. Therefore, the present paper intends to provide guidelines on under what conditions the laser source can be simplified into a surface

or a point source. A novel semi-analytical thermal model is first proposed in which the laser scan vectors are described in terms of point, surface and volumetric sources, respectively. Then the temperature field prediction of these three source geometries will be compared along with the associated computational complexity.

## MODEL DESCRIPTION

A body  $V$  is considered that has already been built and a thin layer of powder is laid on its top surface  $\partial V_{\text{top}}$ , see Fig.1a. The temperature field  $T$  of the body  $V$  is dictated by the heat equation

$$\rho c_p \frac{\partial T}{\partial t} = \nabla \cdot (k \nabla T) + Q_v, \quad \text{in } V, \quad (1)$$

where  $t$  is the time and  $Q_v$  is the rate of volumetric heat generation, i.e. the heat source term. Thermal parameters  $k, \rho, c_p$  are the conductivity, constant-pressure specific heat and density, respectively. For the built body  $V$ , the lateral surface  $\partial V_{\text{lat}}$  and top surface  $\partial V_{\text{top}}$  are covered by the powder, as shown in fig.1a. Upon neglecting convection and radiation effects and considering the fact that the conductivity of the powder is approximately 1/100 of that of the solid body [6], it is reasonable to assume there is no heat flux neither across the lateral surface  $\partial V_{\text{lat}}$  nor across top surface  $\partial V_{\text{top}}$ . The bottom surface  $\partial V_{\text{bot}}$  of body  $V$  is assumed to have the same temperature of the baseplate, which is kept constant during the SLM process.

If the thermal material properties  $k, \rho, c_p$  are assumed to be constant, Eq.(1) will become the linear heat equation. Thus, the scanning line shown in Fig.1a can be discretised by a finite number of heat sources, and the overall temperature field can be obtained by the superposition principle. By performing such discretisation, the thermal influence of each type of heat source can be taken into account individually. The total temperature field is expressed as

$$T = \tilde{T} + \check{T} + \hat{T}, \quad (2)$$

where  $\tilde{T}$  is the temperature due to all heat sources in a semi-infinite space bounded by the top surface of the body  $\partial V_{\text{top}}$ , and obtained by the summation over sources, which reads

$$\tilde{T} = \sum_{I=1}^M \tilde{T}^{(I)}, \quad (3)$$

where  $T^{(I)}$  represents the temperature field due to source  $I$  and  $M$  is the total number of heat sources. The  $\check{T}$  field shown in Eq. (2) is the contribution of image sources, that are positioned as the mirror image of a regular heat source with respect to a boundary, when a given regular source is in the vicinity of the boundary as shown in Fig.1b. The boundary conditions is finally corrected by  $\hat{T}$ . The  $\tilde{T}$  and  $\check{T}$  fields can be obtained directly using analytical expressions while the  $\hat{T}$  field is solved using a numerical method since it is a smooth field. By doing such decomposition, the steep temperature gradients in the vicinity of the laser is captured by the  $\tilde{T}$  and  $\check{T}$  fields, and a boundary value problem (BVP) can be solved for the smooth  $\hat{T}$  field using the boundary conditions of the problem.

For an instantaneous point source in a semi-infinite space, Eq.(1) has the analytical solution[7]

$$\tilde{T}_p(x_i, t) = \frac{QA}{4\rho c_p (\pi\alpha(t-t_0))^{3/2}} \exp\left(-\frac{U^2}{4\alpha(t-t_0)}\right), \quad (4)$$

where  $\tilde{T}_p$  is the temperature field for the point source,  $Q$  represents the energy associated with the heat source while  $A$  is the absorptivity and  $\alpha = k/\rho c_p$  is the thermal diffusivity. The distance between the material point of interest  $x_i$  and the point source position is represented by  $U$ . If the number sources used discretising a scanning line is sufficiently big, the energy  $Q$  can be approximated by  $Q = P\Delta t$ , where  $P$  is the power of the laser and  $\Delta t$  is the time between activation of two consecutive sources.

For a surface source where the total energy  $Q$  associated with the source is distributed as a Gaussian function with the intensity expressed as

$$Q_{ps}^G = \frac{2Q}{\pi r_l^2} \exp\left(\frac{-2r^2}{r_l^2}\right), \quad (5)$$

where  $r_l$  is the radius of the surface source and  $r$  is the distance to the center of the laser. At  $r = r_l$ , the intensity of the Gaussian laser beam reduces to  $1/e^2$  of the maximum intensity. Hence the energy within a radius of  $r_l$  is  $(1-1/e^2)Q$ .

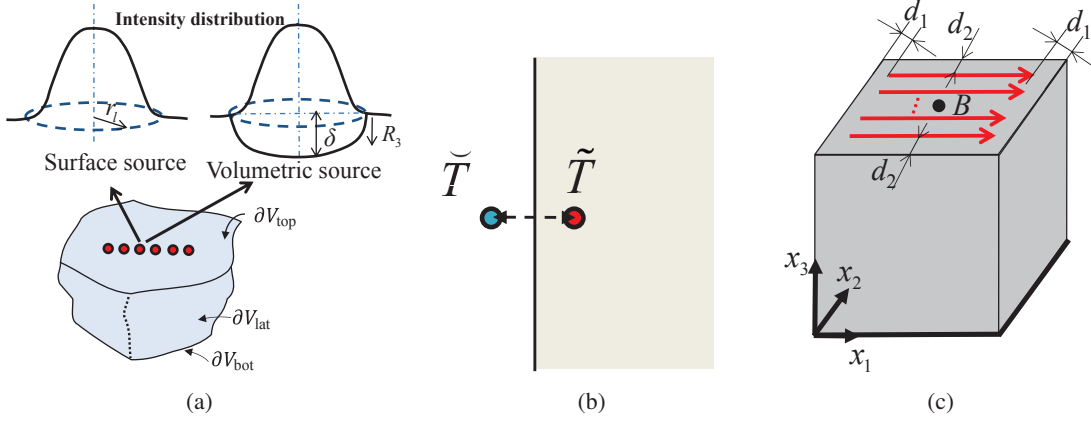


FIGURE 1: (a) The scanning line on the top surface of the already built body can be described by multiple type of heat sources, and each heat source can be considered as a dimensionless point source, a 2D surface source or a 3D volumetric source. (b) Schematic illustration of the image source method (c) A unidirectional scanning pattern with 20 tracks is applied on the top surface of an already built cube.

The temperature field for the surface heat source can then be obtained by substituting Eq. (5) multiplied with  $\omega = e^2/(e^2 - 1)$  into Eq. (4) and integrating the temperature over the area

$$\tilde{T}_{(s)} = \int_0^{r_1} \int_0^{2\pi} \omega \frac{2Q}{\pi r_1^2} \exp\left(-\frac{2r^2}{r_1^2}\right) \frac{\exp\left(\frac{-(U)^2}{4\alpha(t-t_0)}\right)}{4\rho c_p (\pi\alpha(t-t_0))^{3/2}} r d\theta dr. \quad (6)$$

If the laser is considered as a volumetric source, the intensity of the heat source is assumed to satisfy the Beer-Lambert law[8]

$$Q_{pv} = \frac{Q_{ps}^G}{\delta} \exp\left(-\frac{U_3}{\delta}\right), \quad (7)$$

where  $\delta$  is the penetration depth, which is defined as the depth at which the intensity of the radiation inside the material drops to  $1/e$ . The distance  $U_3$  represents the depth value of the volumetric source, as shown in Fig.1a. Similar to the factor  $\omega$  used in Eq. (6), a factor  $\zeta$  is used to make up for the loss of the energy. The absorptivity by the interaction of the laser source and the powder bed is thus given by

$$A = \zeta \int_0^\delta \frac{\exp\left(-\frac{U_3}{\delta}\right)}{\delta} dU_3 = \zeta \left(1 - \frac{1}{e}\right). \quad (8)$$

Substituting Eq.(7) into Eq.(4) and integrating over volume of the source gives

$$\tilde{T}_{(v)} = \zeta \int_0^\delta \int_0^{r_1} \int_0^{2\pi} Q_{pv} \frac{\exp\left(\frac{-(U)^2}{4\alpha(t-t_0)}\right)}{4\rho c_p (\pi\alpha(t-t_0))^{3/2}} r d\theta dr dx_3. \quad (9)$$

## PROBLEM DESCRIPTION

A  $2 \text{ mm} \times 2 \text{ mm} \times 2 \text{ mm}$  cube comprises of Ti-6Al-4V alloy is considered that has already been built by SLM. An additional layer by applying a scanning pattern with 20 unidirectional tracks is analysed, as shown in Fig.1c. The material properties and SLM processing parameters used are tabulated in Table 1 and Table 2, respectively. The hatch spacing is the distance between two adjacent scanning lines and the border offset  $d_1$  and  $d_2$  are shown in Fig.1a. The time step is  $1 \times 10^{-4}$  s. Image source is added when the distance of the laser to a boundary is smaller than the critical distance taken to be 0.75 mm. The bottom surface of the cube is maintained at  $200 \text{ }^\circ\text{C}$ . An 8 noded hexahedral finite difference cells with uniform size of 0.5 mm is used to obtain the  $\hat{T}$  field, and then for any point of interest  $x_i$ , the value of  $\hat{T}(x_i)$  is estimated by the linear interpolation.

TABLE 1: The SLM processing parameters

Laser power $P$ (W)	Laser speed $v$ (m/s)	Border offset $d_1$ (mm)	Border offset $d_2$ (mm)	Hatch spacing $h$ ( $\mu\text{m/s}$ )	Absorptivity $A$ (-)
35	0.3	0.1	0.24	80	0.8

TABLE 2: Material properties [9]

Conductivity $k$ (W/mK)	Heat capacity $c_p$ (J/kgK)	Density $\rho$ ( $\text{g/cm}^3$ )
42	831	4.42

## RESULTS & DISCUSSIONS

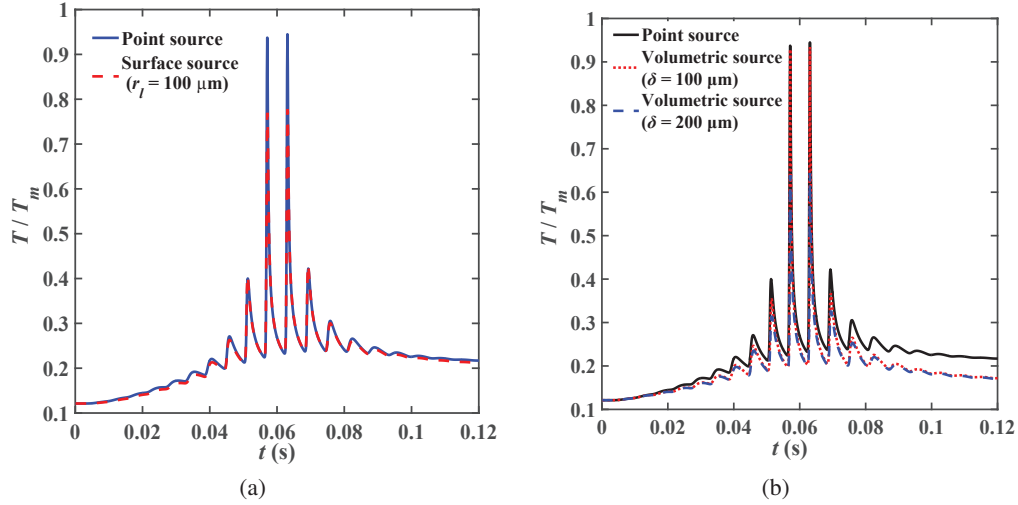


FIGURE 2: Comparison of the normalised temperature history of point  $B$  predicted by the (a) point source model and surface source model with a radius of  $100 \mu\text{m}$  (b) point source model and the volumetric source model with a radius of  $35 \mu\text{m}$ , and two values of penetration depth are taken as  $50 \mu\text{m}$  and  $100 \mu\text{m}$ . The temperature  $T_m$  is the melting point, while  $T$  is the temperature predicted by the proposed model.

The temperature history of point  $B$ , which is at the center of the top surface as shown in Fig.1c, is first used to compare the laser source geometries. In Fig.2, the temperature normalised with melting point  $T_m$ , i.e.  $T/T_m$ , as a function of the scanning time is plotted. The temperature  $T$  is calculated by the proposed model. It can be seen from Fig.2a that when the laser source is modelled as a set of surface sources each with a radius of  $100 \mu\text{m}$ , except the peak value, the temperature history of point  $B$  is very similar to that predicted by the point source model. The considerable difference between the peak temperature values arises when the laser is close to the point  $B$  ( $t = 0.057 \text{ s}$  and  $0.063 \text{ s}$ ). This means the change of the laser radius has little influence on the temperature of the material that is far from the laser. When the radius of the surface source increases, the predicted peak temperature decreases. Similarly, if the radius of the surface source is reduced, the peak temperature predicted by the surface source model increases and converges to the peak value predicted by the point source model when the laser radius is approximately  $35 \mu\text{m}$ .

When modelling the laser scanning vectors with a set of volumetric sources, the laser spot radius is set to be  $35 \mu\text{m}$  in order to isolate the effect of penetration. The penetration depth is assumed to be  $100 \mu\text{m}$  and  $200 \mu\text{m}$ . The difference in the temperature history of point  $B$  obtained by the point and volumetric source models can be clearly observed in Fig.2b. The temperature predicted by the volumetric sources is smaller than that predicted by the point source. Besides, for the volumetric source, the higher the penetration depth, the lower of the temperature. Moreover,

the penetration depth has a larger effect for the temperature of the material close to the heat source, which can be clearly observed in Fig.2b by the variance of the peak values predicted by the two volumetric source models with different penetration depth. The more energy-concentrated heat leads to higher temperature.

Fig.3a - c shows the normalised temperature field of the top surface ( $x_3 = 2$  mm) when the laser arrives at the end of the 10th track ( $t = 0.06$  s). For the surface source, the radius is  $100 \mu\text{m}$ , while for the volumetric source, the radius is  $35 \mu\text{m}$  and the penetration depth is  $100 \mu\text{m}$ . In the vicinity of the laser, temperature decays faster for the volumetric source compared to the surface source. Fig.3d - f show the normalised temperature field of the  $x_1 - x_3$  plane when the laser arrives at the end of the 10<sup>th</sup> track, where  $x_2 = 0.96$  mm. Fig.3d, e and f are the temperature distribution predicted by the point source, surface source and the volumetric source models, respectively. It can be observed that along the thickness direction, the temperature predicted by the point and surface source models are higher than that predicted by the volumetric source model.

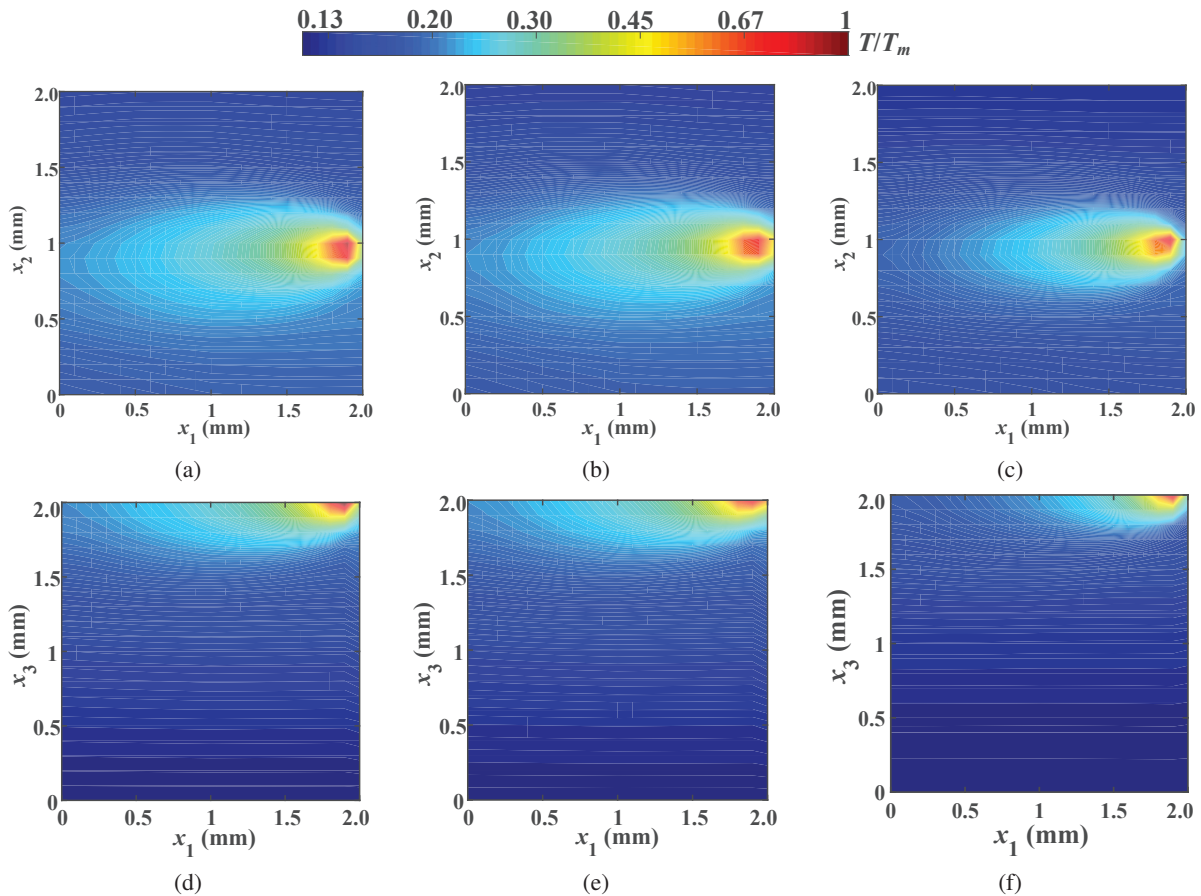


FIGURE 3: Normalised temperature distribution at the end of the 10<sup>th</sup> track on (a)-(c)  $x_1 - x_2$  plane when  $x_3 = 2$  mm, and on (d)-(f)  $x_1 - x_3$  plane when  $x_2 = 0.96$  mm. Temperature field is calculated at (a) and (d) by the point source model, at (b) and (e) by the surface source model with a radius of  $100 \mu\text{m}$  and at (c) and (f) by the volumetric source model with a radius of  $35 \mu\text{m}$  and a penetration depth of  $100 \mu\text{m}$ .

All calculations are performed on a machine with an Intel i7 - 6600U processor with a clock of 2.60 GHz and with 8 GB RAM. The total calculation time for the volumetric, surface and point source are 502.1 s, 287.1 s and 9.8 s, respectively.

## CONCLUSIONS

A semi-analytical thermal model for SLM process is employed to describe the laser scanning vectors with point sources, surface sources and volumetric sources with achieving considerable efficiency. By comparing the temperature history and distribution of a body during SLM with different heat source geometries, it is found that when energy is more concentrated, the source can lead to higher temperature. For the processing and material parameters shown in this paper, if the penetration depth is smaller than  $100\ \mu\text{m}$  and the laser spot radius is smaller than  $35\ \mu\text{m}$ , it is reasonable to represent the laser by point sources instead of modelling it in a volumetric source. The semi-analytical thermal model is also computationally least costly when the laser scanning vectors are described by such point sources.

In the present paper, results are reported for a small cube for simplicity. Upon considering a part with a complex geometry the image field considerations is more complicated and we anticipate the boundary conditions to be imposed by  $\hat{T}$  fields only. Although this will increase the computational cost, the cost is still cheaper than using the finite element scheme directly.

## REFERENCES

- [1] L. Parry, I. A. Ashcroft, and R. D. Wildman, *Additive Manufacturing* **12**, 1–15 (2016).
- [2] M. F. Zaeh and G. Branner, *Production Engineering* **4**, 35–45 (2010).
- [3] C. H. Fu and Y. B. Guo, “3-dimensional finite element modeling of selective laser melting ti-6al-4v alloy,” in *Solid Freeform Fabrication Symposium 2014 Proceedings* (2014), pp. 1129–1144.
- [4] M. Matsumoto, M. Shiomi, K. Osakada, and F. Abe, *International Journal of Machine Tools & Manufacture* **42**, 61–67 (2001).
- [5] A. Hussein, L. Hao, C. Yan, and R. Everson, *Materials & Design* **52**, 638–647 (2013).
- [6] A. V. Gusarov, I. Yadroitsev, P. Bertrand, and I. Smurov, *Journal of Heat Transfer* **131**, p. 072101 (2009).
- [7] H. Carslaw and J. Jaeger, in *Conduction of Heat in Solids* (Oxford Science Publications, 1959).
- [8] C. Morsbach, S. Hges, and W. Meiners, *Journal of Laser Applications* **23**, p. 012005 (2011).
- [9] R. T. Mills, “Some words of caution,” in *Recommended Values of Thermophysical Properties for Selected Alloys* (Woodhead Publishing Limited, Materials Park, Ohio, USA, 2002) p. 13.